Progress In Electromagnetics Research M, Vol. 55, 211–219, 2017

Fast and Stable Integration Method for the Aperture Admittance of an Open-Ended Coaxial Probe Terminated into Low-Loss Dielectrics

Licheng Zhou[1], Yang Ju[2], Peiyu Wang[3], and Yongmao Pei[3, *]

Abstract—The utilization of an open-ended coaxial probe for characterization of dielectric properties or quantitative nondestructive detection of defects in materials firstly requires evaluating the aperture admittance. For the case that the probe is terminated into low-loss dielectrics backed by a conducting sheet, however, the admittance expression encounters poles in the vicinity of the path of integration, resulting in low convergence rate or even overflow in numerical quadrature. In this study, locations and properties of the singularities of the integral formulation for generally lossy, low-loss, and lossless dielectric slabs backed by a perfectly conducting sheet are investigated above all. Subsequently, making use of the contour integral technique, a fast and stable integration method is put forward to calculate the admittance integral formulation. Finally, numerical experiments are conducted to justify the validity and efficiency of the proposed integration method for low-loss dielectric cases by comparison with the traditional integration method as well as commercial FEM software.

1. INTRODUCTION

Open-ended coaxial probes have been extensively used for characterization of dielectric properties and nondestructive detection of defects in materials, owing to their capability of broadband measurement at microwave frequencies along with relatively high spatial resolution [1–5]. Information about the materials under test (MUT), such as complex dielectric properties, thickness of thin dielectric slabs, and disbond in layered media, can be extracted from the reflected microwaves inside the coax [3–8]. These features have made coaxial probes as useful tools for quantitative testing and nondestructive evaluation in microwave engineering, biomedicine, agriculture, geotechnology, etc. [9–15].

In the procedure of quantitative evaluation, one should at first determine the aperture admittance of an open-ended coaxial probe terminated into different MUTs. Up to now, several techniques have been developed for this purpose, such as analytical analysis, semi-analytical full-wave method, and numerical simulation [16–29]. For the analytical method, it is conventionally assumed a probe flange of an infinite area and only fundamental TEM mode propagation inside the coax [16–18]. Moreover, most of the models studied in these methods pertain to an aperture terminated into an infinite dielectric half-space [8, 30–33]. A more general analytical formulation for the cases of layered media backed by a conducting sheet or an infinite half-space was derived by Bakhtiari et al. [18, 34]. However, the aperture expression confronts poles on the real axis along the path of integration when coping with lossless MUTs [18, 34]. Even for low-loss dielectrics, some of the poles in complex domain are quite close to the positive real axis, leading to the possibility of low convergence rate or overflow error in the integration procedure by traditional integration methods (TIMs) (e.g., Gauss-Legendre method, the midpoint rule, etc.) [18, 38]. One promising approach to resolve this issue is to apply the contour integral technique

Received 6 December 2016, Accepted 25 March 2017, Scheduled 13 April 2017

* Corresponding author: Yongmao Pei (peiym@pku.edu.cn).

[1] School of Civil Engineering and Transportation, South China University of Technology, Guangzhou 510641, China. [2] Department of Mechanical Science and Engineering, Nagoya University, Nagoya 464-8603, Japan. [3] State Key Laboratory for Turbulence and Complex Systems, College of Engineering, Peking University, Beijing 100871, China.

(CIT) to calculate the aperture admittance. To the authors' knowledge, however, most of the studies reported in the literature were focused on the cases of generally lossy materials [17–19, 34–37]. In such situations, one can arrive at accurate results for the aperture admittance very efficiently by any traditional numerical integration routine.

In this paper, locations and properties of the singularities of the formulation for the aperture admittance terminated into a conducting sheet backed single-layered dielectric of general loss, low loss, and non-loss are investigated. Based on CIT, a fast and stable numerical method which carries out integration in complex domain is proposed for efficient calculation of the aperture admittance. Numerical simulations are conducted to demonstrate CIT is more stable and efficient when coping with low-loss dielectrics in comparison with TIM as well as commercial FEM software.

2. CIT FOR THE APERTURE ADMITTANCE

Figure 1 depicts the geometry of an open-end coaxial probe with a flange of an infinite diameter terminated into a dielectric slab backed by a perfect conductor. The filling dielectric inside the coax is assumed to have a relative complex permittivity of ε_{rc}. The outer radius of the inner conductor and inner radius of the outer conductor for the coax are denoted by a and b, respectively. A nonmagnetic dielectric slab with relative permittivity $\varepsilon_{r1} = \varepsilon'_{r1} - j \cdot \varepsilon''_{r1}$ and thickness d_1 backed by a conducting sheet is treated as the MUT with infinitely transverse dimensions. Taking into account only the fundamental TEM mode, Bakhtiari et al. [18] derived the terminating admittance normalized with respect to the characteristic admittance of the coax as

$$y_s = \frac{1-R}{1+R} = \int_0^{+\infty} g(\zeta) \cdot f(\zeta)\, d\zeta \tag{1}$$

in which

$$g(\zeta) = \frac{\varepsilon_{r1}}{\sqrt{\varepsilon_{rc}} \ln(b/a)} \cdot \frac{\left[J_0(k_0\zeta b) - J_0(k_0\zeta a)\right]^2}{\zeta} \tag{2}$$

where R refers to the complex reflection coefficient, J_0 the first-kind Bessel function of order zero, and k_0 the wave number in free space. In view of a conducting sheet backed single-layered MUT, the function $f(\zeta)$ in Eq. (1) is in terms of d_1, k_0, and ε_{r1}, and takes the form

$$f(\zeta) = \frac{1}{\sqrt{\varepsilon_{r1} - \zeta^2}} \frac{1}{j \cdot \tan\left(k_0 d_1 \sqrt{\varepsilon_{r1} - \zeta^2}\right)} \tag{3}$$

Conventionally, the dielectric slab in Fig. 1 is replaced with a reference liquid of general loss with well-known dielectric properties, such that the MUT serves as a known load for calibration of the coaxial probe. Under such circumstances, it is quite straightforward and easy to calculate the aperture admittance through Eq. (1) by TIMs, because there are no poles in the vicinity of the positive real axis

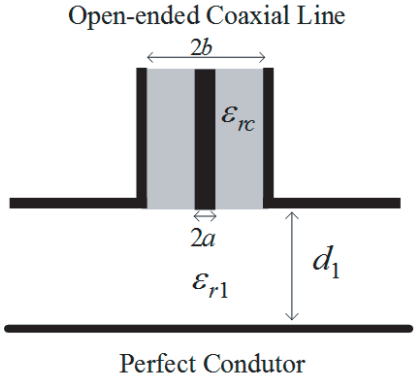

Figure 1. Open-ended coaxial probe terminated into a dielectric slab backed by a perfect conductor.

along the path of integration. As for lossless materials, the path of integration will encounter poles as indicated by Eq. (3). However, most studies were emphasized on MUTs of general loss, and low-loss or lossless dielectrics were not well considered [18, 37]. In this work, we will investigate the locations and properties of the isolated singularities of Eq. (1) for the cases of both $\varepsilon''_{r1} > 0$ and $\varepsilon''_{r1} = 0$, and then put forward a fast and stable integration method based on CIT.

In order to find out the poles, the integrant $g(\zeta) \cdot f(\zeta)$ in Eq. (1) should be investigated. For $g(\zeta)$ as expressed by Eq. (2), there exists a singularity ($\zeta = 0$) on the real axis along the path of integration. However, the limit of $g(\zeta)$ as ζ approaches zero is found to be zero, proving that $\zeta = 0$ is merely a removable singularity [39]. During the numerical integration procedure, the removable singularity $\zeta = 0$ can be ignored. As for $f(\zeta)$ in Eq. (3), one can achieve the locations of the isolated singularities in complex domain by solving the equations $\sqrt{\varepsilon_{r1} - \zeta^2} = 0$ and $\tan(k_0 d_1 \sqrt{\varepsilon_{r1} - \zeta^2}) = 0$, resulting in

$$\zeta_n^s = \sqrt{\varepsilon'_{r1} - [(n\pi)/(k_0 d_1)]^2 - j \cdot \varepsilon''_{r1}} \tag{4}$$

where $n = 0, 1, 2, 3 \ldots$. In consideration of $\varepsilon''_{r1} > 0$ (loss tangent $\tan\delta = \varepsilon''_{r1}/\varepsilon'_{r1} > 0$), all of the singularities ζ_n^s are in the second and fourth quadrants, and none of them falls on the path of integration for Eq. (1).

For the case of low-loss MUTs presented in Fig. 1, the imaginary part of relative permittivity ε''_{r1} and the loss tangent $\tan\delta$ will approach zero. In such a situation, the singularities ζ_n^s tend to be a real number $\sqrt{\varepsilon'_{r1} - [(n\pi)/(k_0 d_1)]^2}$. Considering the dielectric constant should be greater than 1.0, namely $\varepsilon'_{r1} \geq 1.0$, there must exist an integer N satisfying

$$(N \cdot \pi)/(k_0 d_1) \leq \sqrt{\varepsilon'_{r1}} < [(N+1) \cdot \pi]/(k_0 d_1) \tag{5}$$

One can observe that there are $(N + 1)$ singularities near the real axis along the path of integration, and they are close to these points right on the real axis:

$$A_n = \sqrt{\varepsilon'_{r1} - [(n\pi)/(k_0 d_1)]^2} \tag{6}$$

where $n = 0, 1, 2, \ldots, N$. Further inspection of the above equation shows that all of these points A_n on the real axis fall within the interval $[0, A_0]$. In other words, all of the poles are located nearby a segment of the integration path in Eq. (1). If the MUT in Fig. 1 is lossless ($\varepsilon''_{r1} = 0$), the singularities ζ_n^s subsequently can be directly derived from Eq. (4) as $\zeta_n^s = \sqrt{\varepsilon'_{r1} - [(n\pi)/(k_0 d_1)]^2}$, and they are located exactly on the real axis.

The straightforward approach to calculate the terminating admittance expressed by Eq. (1) is to carry out quadrature directly along the positive real axis by TIMs. Since the integral interval ranges from zero to infinite, the integral should be divided into two portions at an interior breakpoint at the first step. For TIM, the integral interval of Eq. (1) can be divided into two portions $C_1 : [0, 2A_0]$ and $C_2 : [2A_0, +\infty]$ as presented in Fig. 2(a). Subsequently, application of transformation of variables [38]

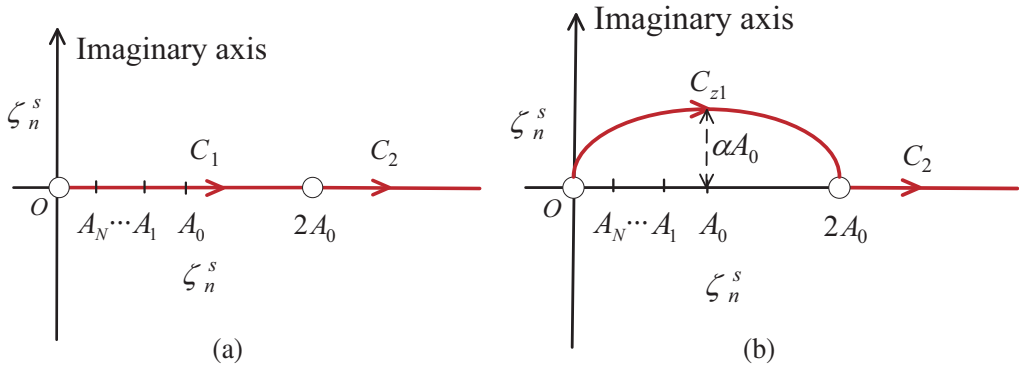

Figure 2. (a) Paths of integration by TIM. (b) Paths of integration by CIT.

on the aperture admittance y_s renders an integral with an integral interval of $[0, 1]$, as expressed by

$$y_s = \int_0^{2A_0} Y_s(\zeta)\, d\zeta + \int_{2A_0}^{+\infty} Y_s(\zeta)\, d\zeta = \int_0^1 \left[2A_0 \cdot Y_s(2A_0 \cdot t) + 2A_0/t^2 \cdot Y_s(2A_0/t)\right] dt \tag{7}$$

in which $Y_s(\zeta) = g(\zeta) \cdot f(\zeta)$. To obtain the numerical results of Eq. (7), one can employ any TIM such as the midpoint rule to readily carry out the integration [38].

As mentioned above, however, there exist $(N + 1)$ isolated singularities that are close to the path $C_1 : [0, 2A_0]$ if the MUT is of low loss. The integral may be difficult to converge to a value with relatively high accuracy when utilizing a TIM to solve it by iteration. Moreover, TIMs are not available to do the integration for the cases of lossless dielectrics due to the existence of singularities on the integrating path. In this study, a fast and stable numerical method based on CIT is proposed to execute the integration for Eq. (1). As described above, the singularities of Eq. (1) fall either within the second and fourth quadrants for the cases of MUTs with loss, or on the real axis for those without loss. This means none of the singularities is located in the first quadrant, indicating that the integrant of Eq. (1) is smooth and analytical in this region. In accordance with Cauchy's theorem [39], the integral along the path $C_1 : [0, 2A_0]$ is equivalent to the one along any path lying within the first quadrant with a starting point at the origin and an ending point at $2A_0$ on the real axis. For the sake of flexibility and simplicity, the integration path in the first quadrant, as presented in Fig. 2(b), can be assumed a semi-ellipse with a center at A_0 and a semi-axis of αA_0 parallel to the imaginary axis. The integration path in the first quadrant is denoted by C_{z1} as depicted in Fig. 2(b), and is expressed as $C_{z1} : z = A_0 + A_0 \cdot (\cos\theta + j\alpha \sin\theta)$ with $\theta \in [\pi, 0]$. Since Bessel functions exhibit a divergence behavior as the imaginary part of the argument increases, it is better to choose $\alpha < 1$ to avoid numerical errors [40]. By using variable substitution, the integral along the path C_1 can be derived as

$$\int_{C_1} Y_s(\zeta)\, d\zeta = \int_{C_{z1}} Y_s(z)\, dz = -\int_0^{\pi} Y_s[z(\theta)]\, dz(\theta) = \int_0^1 \pi A_0 \left[\sin(\pi \cdot t) - j\alpha \cos(\pi \cdot t)\right] \cdot Y_s[z(\pi \cdot t)]\, dt \tag{8}$$

Because no singularity lies in the vicinity of the integration path of C_2, the integral along this path can be operated the same as presented in Eq. (7). Consequently, with the aid of CIT the integral of Eq. (1) finally takes the form

$$y_s = \int_{C_{z1}} Y_s(z)\, dz + \int_{C_2} Y_s(\zeta)\, d\zeta \tag{9}$$

It should be noted that Eq. (9) is applicable to any cases of $\varepsilon''_{r1} \geq 0$, no matter the MUT is of general loss, low loss or non-loss.

3. RESULTS AND DISCUSSION

In this section, a series of numerical simulations will be presented to examine the efficiency and stability of the proposed CIT compared to TIM as well as commercial FEM software. In all the computation cases, the filling material inside the coax depicted in Fig. 1 is assumed to be Teflon with complex dielectric constant $\varepsilon_{rc} = 2.08 \cdot (1 - 0.0006\mathrm{j})$. Dimensions for the coax are chosen as $a = 0.52\,\mathrm{mm}$ and $b = 1.2\,\mathrm{mm}$. Note that the feasible operating frequencies of the coax ranges from DC to 40 GHz.

To begin with, the stability and efficiency of CIT is compared to TIM as the loss tangent of the MUT is varied. In all the simulations, the midpoint rule is adopted as the TIM to calculate the aperture admittance expression of Eq. (7). In this case, the dielectric of the MUT in Fig. 1 is assumed to have a dielectric constant of $\varepsilon'_{r1} = 2.08$ with a thickness of 2.0 mm. The operating frequency is arbitrarily chosen as 10 GHz in the numerical experiments. For both methods, the number of sample points for calculating the integrals of Eq. (7) and Eq. (9) at the first iteration step is chosen as 100, and that of the next ith iteration step would be $100 \cdot 2^{i-1}$. A computational accuracy of 0.0001 is selected as well. Table 1 presents the effect of MUT's loss tangent on the efficiency and stability of the two integration methods as the loss tangent is varied between 10^{-7} and 10^{1}. One may observe from the calculation

results that, for generally lossy cases ($\tan\delta > 10^{-2}$), the iteration steps of CIT and TIM are nearly the same, indicating the two methods yield similar computational efficiency. It can also be seen that the iteration steps are less than 8 for both methods. Clearly, the calculations for MUTs of general loss are easy to converge by either CIT or TIM. As a decrease in the MUT's loss tangent from 10^{-2} to 10^{-5} occurs, however, the iteration steps for TIM substantially increase. As for CIT, those values maintain a constant of 7 as the loss tangent changes from 10^{-2} to 10^{-7}, proving that CIT is less sensitive to low-loss dielectrics and has higher numerical efficiency compared to TIM. Further inspection of the results in the last two rows of Table 1 displays that TIM renders incorrect results as $\tan\delta$ descends to less than 10^{-6}. The problem arises from the existence of the poles in the vicinity of the real axis and resulting overflow error encountered in the computational procedure. As a result, one can infer that the proposed CIT in this study is more stable and efficient than TIM for calculating the coax aperture admittance involving low-loss MUTs.

Table 1. Comparison of the two integration methods for generally lossy and lossless materials.

$\tan\delta$	Integration by Eq. (7) (TIM)		Integration by Eq. (9) (CIT)	
	Iteration Steps	Aperture Admittance	Iteration Steps	Aperture Admittance
10^{1}	7	$1.1279 + 0.0450\text{j}$	7	$1.1279 + 0.0450\text{j}$
10^{0}	7	$0.1245 - 0.1161\text{j}$	7	$0.1245 - 0.1161\text{j}$
10^{-1}	7	$0.0145 - 0.1216\text{j}$	7	$0.0145 - 0.1216\text{j}$
10^{-2}	7	$0.0034 - 0.1220\text{j}$	7	$0.0034 - 0.1220\text{j}$
10^{-3}	8	$0.0023 - 0.1221\text{j}$	7	$0.0023 - 0.1221\text{j}$
10^{-4}	11	$0.0022 - 0.1221\text{j}$	7	$0.0022 - 0.1221\text{j}$
10^{-5}	14	$0.0021 - 0.1221\text{j}$	7	$0.0021 - 0.1221\text{j}$
10^{-6}	7	$0.0000 - 0.1221\text{j}$	7	$0.0021 - 0.1221\text{j}$
10^{-7}	7	$0.0000 - 0.1221\text{j}$	7	$0.0021 - 0.1221\text{j}$

In order to further examine the properties of the proposed CIT in this study, the convergence rate of the two methods at different accuracies is investigated as well. In this case, the calculation parameters depicted in Fig. 1 are chosen as $\varepsilon'_{r1} = 2.08$, $\tan\delta = 10^{-4}$, $d_1 = 2.0\,\text{mm}$ and an operating frequency of 10 GHz. It should be noted that the loss tangent of low-loss materials is typically in the order of 10^{-4}, such as those of quartz and Teflon [41]. The simulation results are shown in Table 2, in which the influence of truncation error from 10^{-4} to 10^{-7} on the convergence rate of the two methods is displayed. One can see that a decrease in truncation error from 10^{-4} to 10^{-7} leads to an increase in the iteration steps for both TIM and CIT. However, CIT requires less iteration steps and computational cost as compared to TIM for the same accuracy. It can be concluded that CIT inherently possesses higher computational efficiency in contrast to traditional integration routine.

Table 2. Efficiency of the two integration methods with diverse computational accuracies.

Truncation Error	Iteration Steps by Eq. (7) (TIM)	Iteration Steps by Eq. (9) (CIT)
10^{-4}	11	7
10^{-5}	11	8
10^{-6}	12	11
10^{-7}	15	15

In the meanwhile, reflection coefficient of three distinct low-loss materials versus frequency in the range of 1 GHz to 40 GHz is calculated by TIM, CIT, as well as the commercial software HFSS. In the numerical simulations, air, Teflon, and quartz are chosen as the low-loss dielectrics with complex dielectric constant $1.0 \cdot (1 - 0.0001\text{j})$, $2.08 \cdot (1 - 0.0006\text{j})$, and $3.82 \cdot (1 - 0.0004\text{j})$, respectively. Each dielectric is assumed to have a similar thickness of 1.0 mm. The simulation results for the three low-loss

MUTs are shown in Fig. 3. Firstly, comparison between TIM and CIT indicates that they render the same calculated values in the whole frequency range for different dielectrics. This is attributed to the same theoretical formulation of Eq. (1) in conjunction with Eqs. (2) and (3) is employed in both TIM and CIT, although the former one executes integration along the real axis whereas the later one does so in complex domain. Calculations by HFSS are also performed to verify the numerical results of the theoretical formulation by TIM and CIT. One may observe from Fig. 3 that the reflection coefficient obtained by TIM and CIT is consistent with that by the FEM software. However, higher frequencies and greater dielectric constant values result in relatively greater difference between the theoretical and FEM results. Nevertheless, the simulations verify the validity and applicability of the proposed CIT for the purpose of broadband measurement. In order to investigate the efficiency, the amount of computational time for the three approaches is counted. In the computations, the reflection coefficient of each dielectric case is calculated in the 1 GHz to 40 GHz range with an interval of 0.5 GHz, namely 79 frequency samples are simulated for each low-loss MUT. The statistic results are displayed in Table 3. It is evident that for all dielectric cases, CIT is the least time-consuming method while FEM software requires maximum computational time. One may see that time cost by TIM is approximately three times larger than that by CIT. For FEM software, a dramatically ascending trend in time consumption is also observed as the dielectric constant raises. In contrast, TIM and CIT exhibit stable time cost for different dielectrics, owing to the fact that they both pertain to analytical methods. As a summary, all the simulation results demonstrate that the proposed CIT in this study has higher efficiency than both TIM and FEM software.

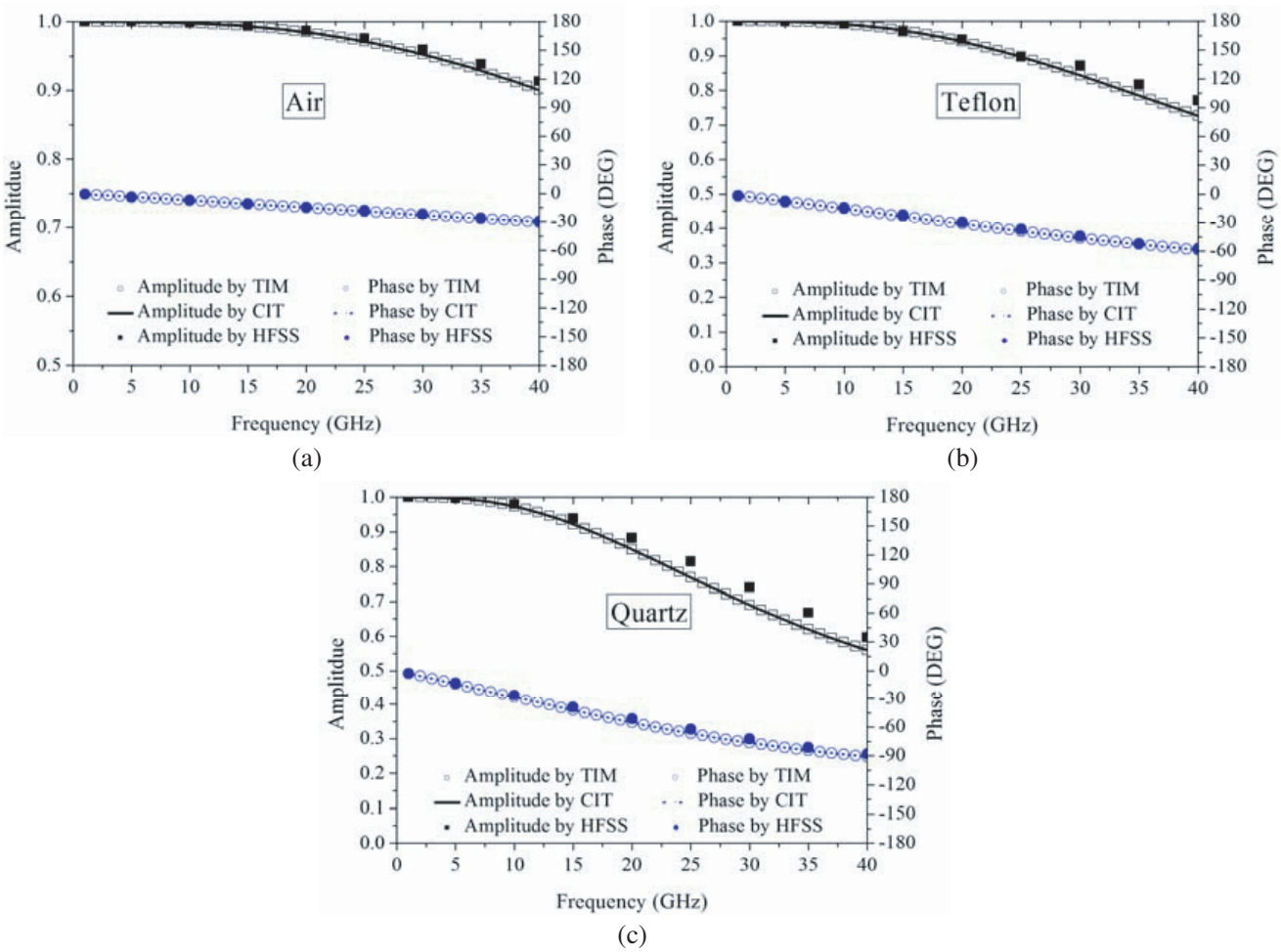

Figure 3. Reflection coefficient amplitude and phase of different dielectrics calculated by TIM, CIT, and HFSS at frequencies ranging from 1 GHz to 40 GHz: (a) air, (b) Teflon, (c) quartz.

Table 3. Computational time cost by TIM, CIT, and HFSS.

Dielectric	Time Cost by TIM	Time Cost by CIT	Time Cost by HFSS
Air	40 s	10 s	1554 s
Teflon	18 s	8 s	7057 s
Quartz	24 s	7 s	9568 s

4. CONCLUSION

The formulation for aperture admittance of an open-ended coaxial probe terminated into low-loss dielectrics backed by a perfectly conducting sheet encounters poles close to the path of integration, leading to low convergence rate or even overflow error in numerical calculations. In this paper, locations and properties of the singularities of the integral for the aperture admittance involving generally lossy, low-loss, and lossless dielectrics are studied. The contour integral method by which the integral is done in complex domain is proposed to calculate the aperture admittance. Numerical calculations demonstrate that the proposed integral method, as compared to traditional integration routines and commercial FEM software, is more stable and efficient for low-loss dielectric cases. The numerical method proposed here can be further used for utilizing an open-ended coaxial probe to fast quantitatively evaluate low-loss dielectrics.

ACKNOWLEDGMENT

This work was supported by the China Postdoctoral Science Foundation (Grant No. 2016M602457), the National Natural Science Foundation of China (Grant Nos. 11522214, 1191216301, 11227801, 11232001, and 11602087), and the Beijing NOVA Program (Grant No. Z151100000315041).

REFERENCES

1. Gregory, A. P. and R. N. Clarke, "A review of RF and microwave techniques for dielectric measurements on polar liquids," *IEEE Trans. Dielectr. Electr. Insul.*, Vol. 13, No. 4, 727–743, Aug. 2006.
2. Pournaropoulos, C. L. and D. K. Misra, "The co-axial aperture electromagnetic sensor and its application in material characterization," *Meas. Sci. Technol.*, Vol. 8, No. 11, 1191–1202, Nov. 1997.
3. Ju, Y., M. Saka, and H. Abé, "Microwave nondestructive detection of delamination in IC packages utilizing open-ended coaxial line sensor technique," *NDT & E Int.*, Vol. 32, No. 5, 259–264, 1999.
4. Ju, Y., M. Saka, and H. Abé, "Detection of delamination in IC packages using the phase of microwaves," *NDT & E Int.*, Vol. 34, No. 1, 49–56, 2001.
5. Ju, Y., M. Saka, and H. Abé, "NDI of delamination in IC packages using millimeter-waves," *IEEE Trans. Instrum. Meas.*, Vol. 50, No. 4, 1019–1023, Aug. 2001.
6. Popovic, D., L. McCartney, C. Beasley, M. Lazebnik, M. Okoniewski, S. Hagness, and J. Booske, "Precision open-ended coaxial probes for in vivo and ex vivo dielectric spectroscopy of biological tissues at microwave frequencies," *IEEE Trans. Microw. Theory Tech.*, Vol. 53, No. 5, 1713–1721, May 2005.
7. Yang, S.-H., K.-B. Kim, and J.-S. Kang, "Detection of surface crack in film-coated metals using an open-ended coaxial line sensor and dual microwave frequencies," *NDT & E Int.*, Vol. 54, 91–95, 2013.
8. Zhang, L., X. Shi, F. You, P. Liu, and X. Dong, "Improved circuit model of open-ended coaxial probe for measurement of the biological tissue dielectric properties between megahertz and gigahertz," *Physiol. Meas.*, Vol. 34, No. 10, N83–N96, Oct. 2013.

9. Athey, T., M. Stuchly, and S. Stuchly, "Measurement of radio frequency permittivity of biological tissues with an open-ended coaxial line: Part I," *IEEE Trans. Microw. Theory Tech.*, Vol. 30, No. 1, 82–86, Jan. 1982.
10. Mehta, P., K. Chand, D. Narayanswamy, D. G. Beetner, R. Zoughi, and W. V. Stoecker, "Microwave reflectometry as a novel diagnostic tool for detection of skin cancers," *IEEE Trans. Instrum. Meas.*, Vol. 55, No. 4, 1309–1316, Aug. 2006.
11. Li, L. L., N. H. Ismael, L. S. Taylor, and C. C. Davis, "Flanged coaxial microwave probes for measuring thin moisture layers," *IEEE Trans. Biomed. Eng.*, Vol. 39, No. 1, 49–57, Jan. 1992.
12. Alanen, E., T. Lahtinen, and J. Nuutinen, "Variational formulation of open-ended coaxial line in contact with layered biological medium," *IEEE Trans. Biomed. Eng.*, Vol. 45, No. 10, 1241–1248, Oct. 1998.
13. Van Damme, S., A. Franchois, D. De Zutter, and L. Taerwe, "Nondestructive determination of the steel fiber content in concrete slabs with an open-ended coaxial probe," *IEEE Trans. Geosci. Remote Sens.*, Vol. 42, No. 11, 2511–2521, Nov. 2004.
14. Wagner, N., M. Schwing, and A. Scheuermann, "Numerical 3-D FEM and experimental analysis of the open-ended coaxial line technique for microwave dielectric spectroscopy on soil," *IEEE Trans. Geosci. Remote Sens.*, Vol. 52, No. 2, 880–893, Feb. 2014.
15. Jiao, X., W. Jin, and X. Yang, "An additional S-shaped structure for sensitivity improvement of coaxial probe for permittivity determination of low loss materials," *Meas. Sci. Technol.*, Vol. 26, No. 5, 055701, May 2015.
16. Mosig, J. R., J. C. E. Besson, M. Gexfabry, and F. E. Gardiol, "Reflection of an open-ended coaxial line and application to nondestructive measurement of materials," *IEEE Trans. Instrum. Meas.*, Vol. 30, No. 1, 46–51, Mar. 1981.
17. Pournaropoulos, C. L. and D. Misra, "A study on the coaxial aperture electromagnetic sensor and its application in material characterization," *IEEE Trans. Instrum. Meas.*, Vol. 43, No. 2, 111–115, Apr. 1994.
18. Bakhtiari, S., S. I. Ganchev, and R. Zoughi, "Analysis of radiation from an open-ended coaxial line into stratified dielectrics," *IEEE Trans. Microw. Theory Tech.*, Vol. 42, No. 7, 1261–1267, Jul. 1994.
19. Qiu, Z., X. Li, and W. Jiang, "On stability of formulation of open-ended coaxial probe for measurement of electromagnetic properties of finite-thickness materials," *Journal of Electromagnetic Waves and Applications*, Vol. 23, No. 4, 501–511, 2009.
20. Li, C. L. and K. M. Chen, "Determination of electromagnetic properties of materials using flanged open-ended coaxial probe-full-wave analysis," *IEEE Trans. Instrum. Meas.*, Vol. 44, No. 1, 19–27, Feb. 1995.
21. Misra, D., "On the measurement of the complex permittivity of materials by an open-ended coaxial probe," *IEEE Microw. Guided Wave Lett.*, Vol. 5, No. 5, 161–163, May 1995.
22. Panariello, G., L. Verolino, and G. Vitolo, "Efficient and accurate full-wave analysis of the open-ended coaxial cable," *IEEE Trans. Microw. Theory Tech.*, Vol. 49, No. 7, 1304–1309, Jul. 2001.
23. Asvestas, J. S., "Radiation of a coaxial line into a half-space," *IEEE Trans. Antennas Propag.*, Vol. 54, No. 6, 1624–1631, Jun. 2006.
24. Okoniewski, M., J. Anderson, E. Okoniewski, K. Caputa, and S. S. Stuchly, "Further analysis of open-ended dielectric sensors," *IEEE Trans. Microw. Theory Tech.*, Vol. 43, No. 8, 1986–1989, Aug. 1995.
25. Hagl, D. A., D. Popovic, S. C. Hagness, J. H. Booske, and M. Okoniewski, "Sensing volume of open-ended coaxial probes for dielectric characterization of breast tissue at microwave frequencies," *IEEE Trans. Microw. Theory Tech.*, Vol. 51, No. 4, 1194–1206, Apr. 2003.
26. Hassan, A. K. A., D. M. Xu, and Y. J. Zhang, "Modeling and analysis of finite-flange open-ended coaxial probe for planar and convex surface coating material testing by FDTD method," *Microw. Opt. Technol. Lett.*, Vol. 24, No. 2, 117–120, Jan. 2000.

27. Hoshina, S., Y. Kanai, and M. Miyakawa, "A numerical study on the measurement region of an open-ended coaxial probe used for complex permittivity measurement," *IEEE Trans. Magn.*, Vol. 37, No. 5, 3311–3314, Sep. 2001.
28. Olmi, R., M. Bini, R. Nesti, G. Pelosi, and C. Riminesi, "Improvement of the permittivity measurement by a 3D full-wave analysis of a finite flanged coaxial probe," *Journal of Electromagnetic Waves and Applications*, Vol. 18, No. 2, 217–232, 2004.
29. Huang, R. and D. Zhang, "Analysis of open-ended coaxial probes by using a two-dimensional finite-difference frequency-domain method," *IEEE Trans. Instrum. Meas.*, Vol. 57, No. 5, 931–939, May 2008.
30. Hilland, J. and T. Friisø, "Evaluation of modelling routines for on-line implementation of the open-ended coaxial probe," *Meas. Sci. Technol.*, Vol. 9, No. 5, 790–796, May 1998.
31. Berube, D., F. M. Ghannouchi, and P. Savard, "A comparative study of four open-ended coaxial probe models for permittivity measurements of lossy dielectric/biological materials at microwave frequencies," *IEEE Trans. Microw. Theory Tech.*, Vol. 44, No. 10, 1928–1934, Oct. 1996.
32. Levine, H. and C. H. Papas, "Theory of the circular diffraction antenna," *J. Appl. Phys.*, Vol. 22, No. 1, 29–43, Jan. 1951.
33. Irzinski, E. P., "The input admittance of a TEM excited annular slot antenna," *IEEE Trans. Antennas propag.*, Vol. 23, No. 6, 829–834, Nov. 1975.
34. Ganchev, S., N. Qaddoumi, S. Bakhtiari, and R. Zoughi, "Calibration and measurement of dielectric properties of finite thickness composite sheets with open-ended coaxial sensors," *IEEE Trans. Instrum. Meas.*, Vol. 44, No. 6, 1023–1029, Dec. 1995.
35. Misra, D., M. Chabra, B. Epstein, M. Mirotznik, and K. Foster, "Noninvasive electrical characterization of materials at microwave frequencies using an open-ended coaxial line: Test of an improved calibration technique," *IEEE Trans. Microwave Theory Tech.*, Vol. 38, 8–14, Jan. 1990.
36. Blackham, D. V. and R. D. Pollard, "An improved technique for permittivity measurements using a coaxial probe," *IEEE Trans. Instrum. Meas.*, Vol. 46, No. 5, 1093–1099, Oct. 1997.
37. Wu, M., X. Yao, J. Zhai, and L. Zhang, "Determination of microwave complex permittivity of particulate materials," *Meas. Sci. Technol.*, Vol. 12, No. 11, 1932–1937, Nov. 2001.
38. Press, W. H., B. P. Flannery, S. A. Teukolsky, and W. T. Vetterling, *Numerical Recipes*, Cambridge University Press, Cambridge, England, 1986.
39. Ahlfors, L. V., *Complex Analysis*, McGraw-Hill, New York, 1979.
40. Gay-Balmaz, P. and J. R. Mosig, "Three-dimensional planar radiating structures in stratified media," *Int. J. Microw. Millimeter-Wave Comput.-Aided Eng.*, Vol. 7, No. 5, 330–343, Sep. 1997.
41. Hollinger, R. D., K. A. Jose, A. Tellakula, V. V. Varadan, and V. K. Varadan, "Microwave characterization of dielectric materials from 8 to 110 GHz using a free-space setup," *Microw. Opt. Technol. Lett.*, Vol. 26, No. 2, 100–105, Jul. 2000.